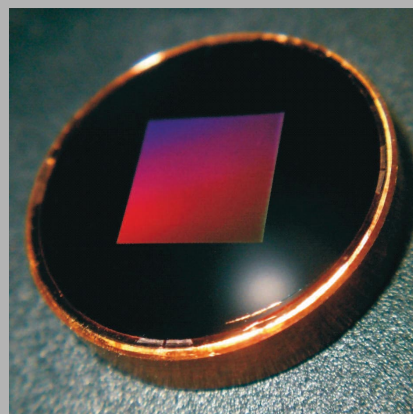


Abstract: We report the first demonstration of resonant-grating-based laser wavelength tuning in the mid-infrared spectral domain and with Littrow mounting of the grating. We show for a mid-infrared Cr:ZnSe laser that this tuning technique is much more wavelength selective than prism-based tuning, while inducing very low cavity losses (around 2%), which are at least two times smaller than in the case of a standard metal grating. Furthermore, the resonant grating allows tuning the Cr:ZnSe laser over as much as 400 nm around a center wavelength of 2.38 μm . This shows the potential of employing Littrow-mounted resonant diffraction gratings for controlling and tuning the emission wavelength of lasers emitting in the mid-infrared spectral domain and other wavelength regions.



Resonant diffraction grating designed for tuning a Cr:ZnSe laser in Littrow configuration

© 2011 by Astro Ltd.

Published exclusively by WILEY-VCH Verlag GmbH & Co. KGaA

Low-loss wavelength tuning of a mid-infrared Cr²⁺:ZnSe laser using a Littrow-mounted resonant diffraction grating

N. Vermeulen,^{1,*} P. Wasylczyk,² S. Tonchev,^{3,#} P. Muys,⁴ H. Ottevaere,¹ O. Parriaux,³ and H. Thienpont¹

¹ Brussels Photonics Team, Dept. Applied Physics and Photonics, Vrije Universiteit Brussel, 1050 Brussels, Belgium

² Institute of Experimental Physics, University of Warsaw, 69, ul. Hoża, 00-681 Warszawa, Poland

³ H. Curien Laboratory UMR CNRS 5516, Lyon University, F-42000 Saint-Etienne, France (#: on leave from the ISSP of the Bulgarian Academy of Sciences)

⁴ Lambda Research Optics Europe, 2, Tulpenstraat, 9810 Eke, Belgium

Received: 8 April 2011, Revised: 12 April 2011, Accepted: 15 April 2011

Published online: 1 June 2011

Key words: laser wavelength tuning; resonant diffraction grating; mid-infrared lasers

1. Introduction

Controlling and tuning the emission wavelength of lasers with a broad gain spectrum has been a widely researched topic already for many decades [1]. Various configurations have been proposed, many of them relying on the implementation of prisms and/or diffraction gratings inside the laser cavity [2, 3]. While the use of prisms is preferred in case low intra-cavity losses are required, one opts for diffraction gratings when a high wavelength selectivity is needed [1]. The possibility of having both low insertion losses and a high wavelength selectivity came within

reach when the first volume Bragg gratings with absolute diffraction efficiencies above 93% were demonstrated in the late 90s [4]. Although very efficient in the visible and near-infrared wavelength domains, these gratings feature a lower performance at mid-infrared wavelengths beyond 2500 nm, as the photo-thermo-refractive glasses they are made of exhibit increasing absorption losses in this spectral domain [4, 5].

A few years ago, it was shown that absolute diffraction efficiencies as high as 99% can be achieved using “resonant” diffraction gratings [6], which can be designed for virtually any wavelength domain. Many of the resonant

* Corresponding author: e-mail: nvermeul@b-phot.org

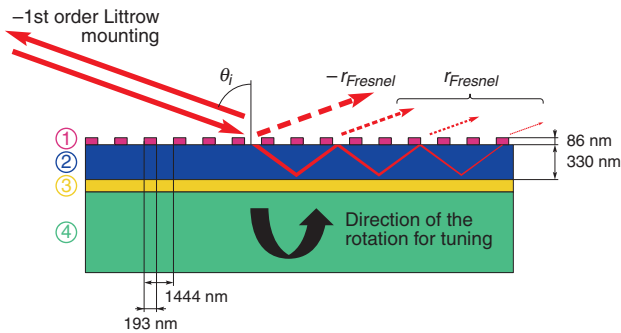


Figure 1 (online color at www.lphys.org) Schematic representation of a resonant diffraction grating designed for intra-cavity tuning of a mid-infrared laser under -1 st order Littrow mounting. Layers 1, 2, 3, and 4 correspond to the Ge grating layer, the ThF_4 layer, the Cu mirror, and the quartz substrate, respectively. The Fresnel reflection is made up of two contributions, namely r_{Fresnel} and $-r_{\text{Fresnel}}$, which cancel out each other through total destructive interference

gratings developed thus far operate along the principle of “resonant reflection,” whereby the incident light excites a guided mode inside the multilayer structure of the grating, which is then reradiated into air in the direction of Fresnel reflection [6]. In 2007, such a “resonant reflection” grating was used for efficient intra-cavity wavelength stabilization and tuning of near-infrared lasers [7]. Because of its operation principle the grating had to be mounted along the Littman-Metcalf configuration with an additional mirror steering the reflected beam back into the laser cavity. An important next step would be to obtain efficient laser wavelength tuning using another type of resonant grating that relies on “resonant diffraction” instead of “resonant reflection” [6] and that can be mounted along the Littrow configuration where no additional mirror is needed. Furthermore, it would be most interesting to examine whether besides near-infrared lasers also mid-infrared lasers could be tuned by means of a resonant grating. Although several types of wavelength-variable mid-infrared laser sources have been developed over the past several years [8–21], the mid-infrared spectral domain is still considered to be an “exotic” spectral region due to the lack of optical components usable at mid-infrared wavelengths. Nevertheless, this spectral region is most promising as it offers a myriad of application potentialities in various domains such as spectroscopy (e.g. trace gas analysis and environmental monitoring) and biomedicine (e.g. microsurgery and optical coherence tomography) [8, 11, 22]. Recently several papers have been published on the design and fabrication of resonant gratings suitable for mid-infrared operation, however, these components lack the high diffraction efficiencies required for obtaining low-loss intra-cavity wavelength tuning [23, 24].

In this paper, we report the first demonstration of resonant-grating-based laser wavelength tuning at mid-

infrared wavelengths and with the grating implemented along the Littrow configuration. We show for a mid-infrared Cr:ZnSe laser that this tuning technique induces only small losses while providing a high wavelength selectivity and a broad tuning range. After discussing the design, fabrication and characterization of the grating, we present the wavelength tuning characteristics obtained for a mid-infrared Cr:ZnSe laser with resonant-grating-based tuning, and compare these characteristics to those measured for prism-based tuning. Finally, we make a performance comparison between our resonant tuning grating and conventional metal tuning gratings.

2. Specifications of the resonant diffraction grating

2.1. Operation principle of the grating

Well after R.W. Wood identified anomalies in the spectra of gratings in 1902 [25], several research groups have investigated practical applications of these phenomena, and as such paved the way to the development and implementation of resonant gratings [26–28]. The type of resonant grating that we consider in this paper establishes resonant diffraction in the -1 st order under Littrow mounting (see Fig. 1). Such a grating can replace one of the end mirrors in a laser cavity, so that the laser wavelength can be tuned by tilting the grating while at the same time a high spectral selectivity is obtained as only one narrow spectral line satisfies the stable mode condition in the laser cavity of fixed geometry.

Unlike conventional -1 st order Littrow gratings that diffract transverse magnetic (TM)-polarized light by a metallic corrugation, the grating under consideration relies on resonant diffraction of the transverse electric (TE) polarization by a composite structure consisting of a non-corrugated metal mirror and a corrugated dielectric superstructure. The general operation principle of such a grating can be understood by first considering a metal mirror covered by a plain dielectric film. When this structure is illuminated by a light wave at an angle of incidence that satisfies the leaky mode dispersion relation given in [6], the incident wave excites through refraction a trapped mode in the dielectric film with some leakage at the film surface [6, 28]. Without corrugation on top of the dielectric film, the Fresnel reflection has two contributions: the light reflected first at the film surface, and the fraction of the trapped leaky mode that reradiates into air. When the dispersion equation is satisfied, i.e., when the leaky mode resonance condition is established, these two contributions to the reflection are phase shifted by π , and thus they interfere destructively. When a periodic corrugation is fabricated on top of the film, its -1 st diffraction order provides under the aforementioned resonance condition an additional output port for the field present in the film. The presence of the corrugation degrades the quality of the resonator

for the trapped mode; this permits to balance the modulus of the two reflection contributions, and thus to cancel out the overall reflection in the Fresnel direction through total destructive interference between the two contributions (see Fig. 1). If the -1 st diffraction order only can propagate (the $+1$ st and -2 nd orders are made evanescent by the choice of the angle of incidence θ_i and the grating period Λ), 100% of the power is diffracted along the -1 st order except the fraction dissipated in the buried mirror. It should be noted that such “resonant diffraction” grating has been used before in [6], but there the purpose was to establish off-Littrow diffraction in the -1 st order. For a grating in -1 st order Littrow mounting as considered here, when the incident beam excites a leaky mode of the grating structure, the -1 st order diffracted beam corresponds to the same leaky mode propagating in the opposite direction. Hence, a double resonance is established. If now such a Littrow-mounted grating is used as an end mirror in a laser resonator, it will act as a standard Littrow grating mirror and reflect incident rays with wavelength $\lambda = 2\Lambda \sin \theta_i$ in the same direction as they originated from.

2.2. Design, fabrication, and characterization of the grating

To design a “resonant diffraction” grating suitable for tuning the wavelength of a mid-infrared laser, we selected quartz as substrate material, copper (Cu) as mirror material, thorium fluoride (ThF_4) as the material for the dielectric film, and germanium (Ge) for fabricating the corrugation on top of the latter (see Fig. 1). ThF_4 and Ge are cohesive materials with a high refractive index difference ($n_f = 1.50$ for ThF_4 versus $n_c = 4.07$ for Ge) so that a high diffraction efficiency can be established with relatively shallow grooves. Furthermore, ThF_4 is transparent from the UV until the far infrared.

To make a resonant grating highly wavelength selective, one has to design it for grazing incidence operation, i.e., for large angles of incidence θ_i (see Fig. 1). As such, we assumed that the light beam incident on the grating – in our case this was the cavity mode of a Cr:ZnSe laser with a nominal center wavelength of $2.5 \mu\text{m}$ – would illuminate the grating at an angle θ_i of 60 degrees. The reason for not choosing a larger angle was that with 60 degrees we still had a sufficiently skew grating positioning to ensure a high wavelength selectivity, while at the same time allowing a broad tuning bandwidth. For a $2.5 \mu\text{m}$ light beam incident at an angle of 60 degrees, the grating period $\Lambda = \lambda / (2 \sin \theta_i)$ should be 1444 nm. Furthermore, to establish the fundamental leaky mode inside the grating structure for this beam, the total phase shift of the trapped TE wave, which comprises the shift $2k_0 n_f \cos \theta_f$ for one round trip in the dielectric film ($k_0 = 2\pi/\lambda$ and θ_f is the angle of refraction in the film) and the reflection phase shifts at the air side and at the metal side (0 and $\sim \pi$, respectively), must be equal to 2π . This implies that the dielec-

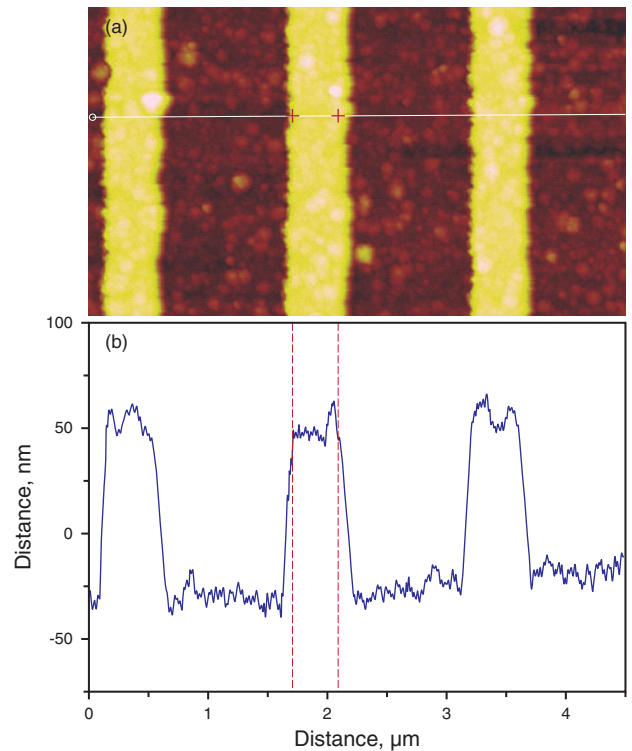


Figure 2 (online color at www.lphys.org) AFM scan of the fabricated resonant grating. (a) – 2D image of the grating from above and (b) – cross-sectional height variations

tric layer thickness together with the corrugation equivalent thickness should be close to a quarter wavelength [6]. This thickness estimate was then implemented in an optimization code, which determines the exact layer thickness and grating depth yielding maximum diffraction efficiency, while using the grating duty cycle as an optimization variable. The optimized thicknesses of the dielectric film and the grating layer were 330 and 86 nm, respectively (see Fig. 1). These thicknesses in combination with a small duty cycle of 0.15 (line/space ratio of $\sim 1/6$) could yield diffraction efficiencies between 97% and 100% for angles of incidence ranging from 52 to 75 degrees, covering the wavelength range between 2.3 to 2.8 μm .

After depositing the ThF_4 and Ge coatings on the Cu substrate by thermal evaporation, we transferred a chromium grating mask, made by a laser pattern generator, into a photoresist layer by means of a hard-contact photolithographic mask transfer under mercury lamp exposure. Then, we transferred the corrugation into and all through the Ge layer by wet etching. The advantage of using wet etching was that the associated underetching enabled us to obtain a small duty cycle, with the ThF_4 layer surface acting as an etch stop.

After fabrication, we first characterized the grating morphology using an atomic force microscope (AFM). As can be seen in the AFM scan shown in Fig. 2, the actual

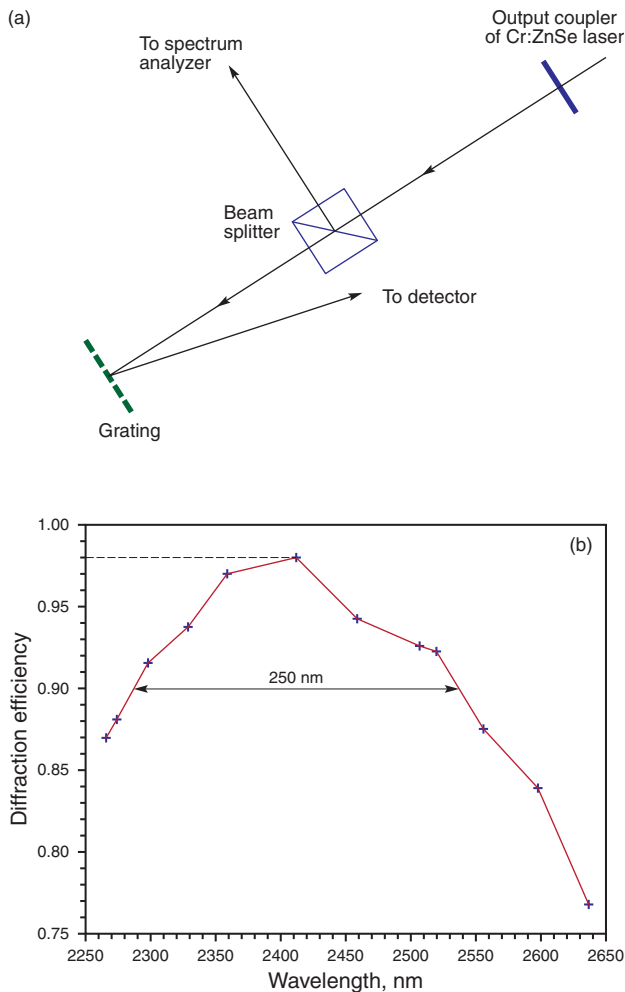


Figure 3 (online color at www.lphys.org) Diffraction efficiency of the resonant grating. (a) – top view of the measurement setup and (b) – measured diffraction efficiencies as a function of wavelength

grating duty cycle, the grating period, and the thickness of the Ge layer were around 0.25, 1480 nm, and 78 nm, respectively. Only for the duty cycle there was a substantial deviation between the actual and targeted value (0.25 *versus* 0.15), but still the fabrication could be considered as successful since achieving small duty cycles is challenging in practice and no specific technology development was intended at this stage.

Secondly, we characterized the absolute diffraction efficiency of the grating in the spectral range around 2.5 μm . Hereto, we illuminated the grating with the output beam of a Cr:ZnSe laser, in which a prism was implemented as tuning element – the laser configuration is described in detail in the following section – and we positioned the grating such that the groove lines were parallel to the TE polarization direction of the laser light and a small horizontal offset

was induced between the propagation directions of the incident and reflected light beams (see Fig. 3a). The latter enabled us to measure the reflected power without interfering with the incident power. Then, we vertically rotated the grating until the reflected beam was at the same height as the incident beam, as is required for intra-cavity operation; like one would expect for a properly designed grating, this operation point maximized the reflected power. The highest ratio of reflected power to incident power, i.e., the highest diffraction efficiency, was obtained for the wavelength of 2.41 μm at an angle of incidence around 60 degrees and was as high as 98% (see Fig. 3b). The diffraction efficiency remained above 90% over a wavelength range of 250 nm and for angles of incidence between approximately 55 and 65 degrees. The reason for not having a maximal diffraction efficiency at 2.5 μm – the nominal design wavelength – was that in the fabricated grating structure the leaky mode condition was not exactly satisfied at this wavelength. The reduction in tuning range compared to what we had calculated before was due to the difference between the targeted and actual grating duty cycles. Nevertheless, the data presented in Fig. 3b confirm that a resonant grating can achieve both high diffraction efficiencies and a relatively broad operation bandwidth, and with improved control of the layer thickness and grating duty cycle even better results could be obtained. This underlines the assets a resonant diffraction grating can offer when used as an intra-cavity laser tuning element (see next section).

3. Tuning a Cr²⁺:ZnSe laser with a resonant diffraction grating

3.1. Resonant diffraction grating versus prism as tuning element

This section focuses on the performance of our resonant grating as a tuning element for a mid-infrared Cr:ZnSe laser, a type of laser which belongs to the category of transition-metal-doped chalcogenide lasers. Over the past several years, much progress has been made in the development of tunable mid-infrared transition-metal-doped chalcogenide lasers, featuring various cavity designs and pumping schemes and with operation in the continuous-wave regime and in the pulsed regime [13–21]. The resulting laser configurations have already yielded excellent performance and lasing efficiencies. In this paper, rather than fixing attention on lasing efficiencies as such, the focus is on the efficiency of resonant-grating-based wavelength tuning. As will be discussed in the following sections, this tuning technique has significant advantages compared to other tuning approaches, and hence has the potential of taking the overall performance of the tunable laser configurations referred to above to an even higher level.

The laser which we used to evaluate the tuning performance of our resonant grating was a continuous-wave

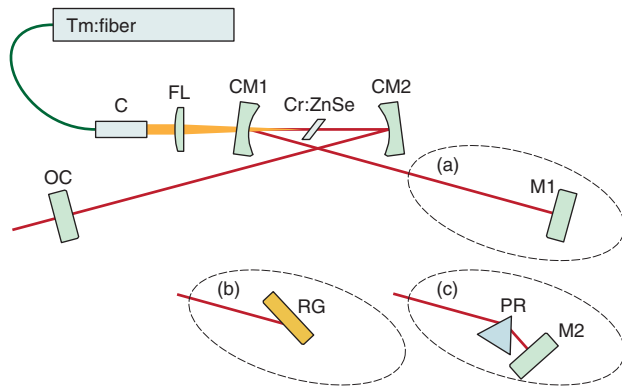


Figure 4 (online color at www.lphys.org) Schematic representation of the Cr:ZnSe laser configuration. (a) – without tuning element, (b) – with the resonant diffraction grating as tuning element, (c) – with a prism as tuning element. The specifications of the different components in the cavity are: Tm:fiber – continuous-wave Thulium-doped-fiber pump laser, C – fiber collimator, FL – focusing lens ($f = 100$ mm), CM1,2 – concave mirrors (radius of curvature = 100 mm), Cr:ZnSe – Brewster-cut laser crystal, OC – output coupler, M1,2 – flat high-reflection mirror, RG – resonant diffraction grating, and PR – Brewster-cut MgF_2 prism

Cr:ZnSe laser with an X-shaped cavity (see Fig. 4). To benchmark the grating's performance, we also made a comparison with the case where a Brewster-cut MgF_2 prism was employed to tune the laser. In the X-shaped cavity, spectral tuning was provided by replacing the high-reflection (HR) end mirror by the resonant grating or by the prism and an additional HR mirror (see Fig. 4b and Fig. 4c, respectively). We implemented the Cr:ZnSe crystal (optical length: 10 mm, absorption coefficient: 1.18 cm^{-1} , and provider: North Crystals America) at Brewster angle, hence yielding TE-polarized lasing radiation. The laser was pumped with a continuous-wave Tm-doped fiber laser at $1.8 \mu\text{m}$. To minimize the total intra-cavity losses for the spectral tuning measurements, we used a low-transmission output coupler (3% transmission). The pump power incident on the Cr:ZnSe crystal was 2.25 W, a value significantly above the lasing threshold but still low enough to ensure a stable laser spectrum with both tuning techniques [13].

Fig. 5 shows the measured laser output power as a function of emission wavelength, when the laser was tuned using either the resonant diffraction grating or the prism. The highest-power emission wavelength – $2.52 \mu\text{m}$ without tuning element – was shifted towards 2.38 and $2.35 \mu\text{m}$ upon insertion of the resonant grating and the prism, respectively. Although the measured tuning range of the resonant grating is 30% smaller than that of the prism, it still spans over 400 nm between 2.23 and $2.63 \mu\text{m}$. The short-wavelength limit is not determined by the grating's operation bandwidth but by the decrease in reflectivity of the cavity mirrors when moving towards shorter

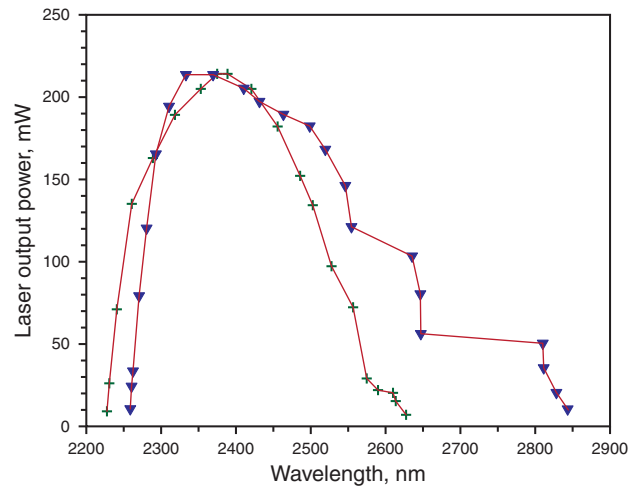


Figure 5 (online color at www.lphys.org) Measured tuning curves for the Cr:ZnSe laser with resonant-grating-based (+) and prism-based (∇) tuning

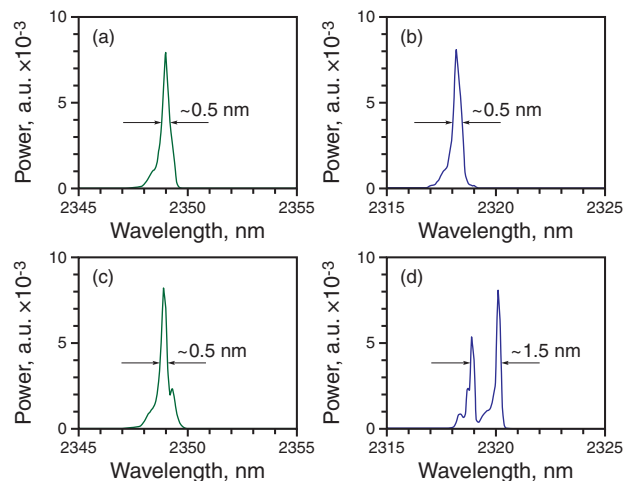


Figure 6 (online color at www.lphys.org) Laser spectra obtained for: (a),(c) – resonant-grating-based tuning at laser output powers around 200 and 480 mW, respectively; (b),(d) – prism-based tuning at laser output powers around 200 and 480 mW, respectively

wavelengths. Fig. 5 also shows that the absolute laser output powers measured at the respective optimal emission wavelengths are approximately equal for both tuning techniques. Since the insertion losses of Brewster-cut tuning prisms are known to be very low [14], the latter confirms that the diffraction efficiency of the resonant grating is very high and its losses small.

Regarding the spectral line shape, for a moderate pump power of 2.25 W and a laser output power around 200 mW, the laser spectra exhibited approximately the same shape for both tuning techniques, and featured a FWHM linewidth of about 0.5 nm (see Fig. 6a and

Fig. 6b). However, for significantly higher pump powers, we observed unstable and broader laser spectra with the prism, while the spectra with the resonant-grating-based tuning remained stable and narrow. For a pump power of 4.7 W and a laser output power around 480 mW, we measured a constantly changing, 1.5 nm wide, split spectrum for the prism-based setup, while for the grating-based configuration a stable and 3 times narrower spectrum with a FWHM linewidth of 0.5 nm was recorded (see Fig. 6c and Fig. 6d). The strong wavelength selectivity of the resonant grating thus enables us to enforce lasing at a fixed wavelength and hence to stabilize the lasing wavelength much better than when using prism-based tuning.

3.2. Resonant diffraction grating versus metal diffraction grating as tuning element

To benchmark the tuning performance of our resonant grating with that of a metal grating, we compared our results to those obtained recently by I.S. Moskalev et al. [20] for a mid-infrared Cr:ZnSe laser tuned with such a metal grating also in the Littrow configuration. They demonstrated a tuning range spanning the 1950–2800 nm band, approximately two times wider than what we obtained with the resonant grating. The wider tunability they achieved at the short-wavelength side is, however, mainly due to the broader bandwidth of the cavity mirrors in their laser setup. Because of the resonant nature of our resonant grating, its operation bandwidth is de facto smaller than that of a metal grating, but thanks to its higher diffraction efficiency (98% versus 95% for the metal grating in [20]), it also gives rise to substantially lower insertion losses in the laser cavity (2% versus 5% for the metal grating).

To estimate the effect of such a difference in insertion loss on the attainable laser output power, we compared the output power decrease for our laser setup upon insertion of the resonant grating to the output power decrease recorded by I.S. Moskalev et al. upon insertion of their metal grating. The metal grating in the high-power laser setup of I.S. Moskalev et al. caused the laser output power to drop from 10.5 to 7.4 W, i.e., a decrease of more than 3 W, when using a 26.9% output coupler [20]. To make a valid comparison with the output power decrease induced by our resonant grating, we replaced in our laser cavity the 3% output coupler by a 17% output coupler, and we measured the input-output power curves of the laser before and after replacing the HR end mirror by the resonant grating. As shown by Fig. 7, the slope efficiencies of the measured input-output curves are approximately equal, i.e., around 24%. This result is in line with J.A. Caird's analysis [29], which says that the ratio of the slope efficiencies, under the assumption that the HR end mirror is lossless, should correspond to

$$\frac{\ln(1 - 0.17)}{\ln(1 - 0.17) - 0.02} = 0.903,$$

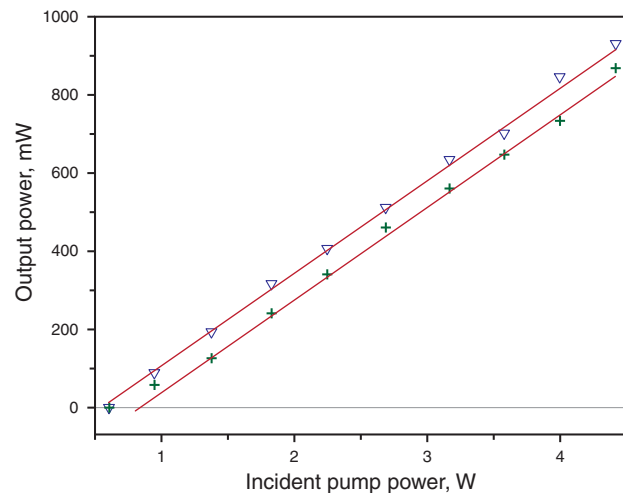


Figure 7 (online color at www.lphys.org) Input-output power curves for the Cr:ZnSe laser with (+) and without (▽) the resonant diffraction grating replacing the HR end mirror. The lines are linear fits, indicating a slope efficiency around 24% for both configurations

whereby the numbers 0.17 and 0.02 indicate the output coupler transmission and the grating's insertion loss at the wavelength of 2.41 μm , respectively. Due to the approximate equality of the slope efficiencies, there is a fixed power offset between the two curves of about 70 mW. Hence, in principle, one would have a resonant-grating-induced power decrease of 70 mW also when operating the laser at the same high power levels as in [20], and this power loss is more than 40 times smaller than the ca. 3 W power loss reported in [20]. Important to note is that in the Cr:ZnSe laser setup of C.H. Zhang et al. where a volume Bragg grating was inserted just to establish narrow-linewidth operation without wavelength tuning [19] the corresponding power loss was also significantly larger than the power loss we observed for our resonant grating (540 versus 70 mW). Of course, the comparison we made here with the results for the metal tuning grating of I.S. Moskalev et al. [20] is only a theoretical first-order comparison, which we are not able to verify experimentally since our pump laser is not powerful enough to generate the same high output powers as in [20]. Nevertheless, we can safely say that with resonant tuning gratings a dramatic improvement in lasing efficiency can be established as compared to metal tuning gratings.

4. Conclusion

We demonstrated low-loss, high-selectivity wavelength tuning of a mid-infrared Cr:ZnSe laser using a resonant diffraction grating under Littrow mounting. The grating was designed and fabricated to achieve a high diffraction

efficiency, high wavelength specificity and a broad tuning bandwidth. When optimizing the manufacturing process for a more precise control of the layer thicknesses and the grating duty cycle, even better results could be obtained. Hence, resonant diffraction gratings have the potential of becoming one of the best performing wavelength tuning elements for lasers operating in the mid-infrared wavelength region and in other wavelength domains.

Acknowledgements This work is financially supported in part by FWO-Vlaanderen, which provides a Postdoctoral Research grant for N. Vermeulen, and in part by Belgian Science Policy – Interuniversity Attraction Poles, VUB – Geconcerteerde OnderzoeksActie, VUB – Onderzoeksraad, the Industrial Research Fund, the Flemish Methusalem Programme, and the EC-funded FP6 Network of Excellence on Micro-Optics (NEMO).

References

- [1] F.J. Duarte, *Tunable Laser Optics* (Academic, New York, 2003), chap. 2.
- [2] F.C. Strome, Jr. and J.P. Webb, *Appl. Opt.* **10**, 1348–1353 (1971).
- [3] E.E. Marinero, A.M. Angus, and M.J. Colles, *Opt. Commun.* **14**, 226–228 (1975).
- [4] O.M. Efimov, L.B. Glebov, L.N. Glebova, K.C. Richardson, and V.I. Smirnov, *Appl. Opt.* **38**, 619–627 (1999).
- [5] L.B. Glebov, *Proc. SPIE* **6216**, 621601 (2006).
- [6] N. Destouches, A. Tishchenko, J. Pommier, S. Reynaud, O. Parriaux, S. Tonchev, and M. Ahmed, *Opt. Express* **13**, 3230–3235 (2005).
- [7] S. Giet, C.-L. Lee, S. Calvez, M.D. Dawson, N. Destouches, J.-C. Pommier, and O. Parriaux, *Opt. Express* **15**, 16520–16526 (2007).
- [8] I.T. Sorokina and K.L. Vodopyanov (eds.), *Solid-State Mid-Infrared Laser Sources* (Springer-Verlag, Berlin – Heidelberg, 2003), pp. 445–538.
- [9] W. Lei and C. Jagadish, *J. Appl. Phys.* **104**, 091101 (2008).
- [10] T.-J. Wang, H.-Z. Zhang, F.-G. Wu, Z.-S. Feng, H.-Y. Zang, Z.-H. Kang, Y. Jiang, and J.-Y. Gao, *Laser Phys.* **19**, 377–380 (2009).
- [11] M. Skorczakowski, J. Swiderski, W. Pichola, P. Nyga, A. Zajac, M. Maciejewska, L. Galecki, J. Kasprzak, S. Gross, A. Heinrich, and T. Bragagna, *Laser Phys. Lett.* **7**, 498–504 (2010).
- [12] B.M. Walsh, *Laser Phys.* **20**, 622–634 (2010).
- [13] E. Sorokin, S. Naumov, and I.T. Sorokina, *IEEE J. Sel. Top. Quantum Electron.* **11**, 690–712 (2005).
- [14] A. Sennaroglu, U. Demirbas, N. Vermeulen, H. Ottevaere, and H. Thienpont, *Opt. Commun.* **268**, 115–120 (2006).
- [15] M.E. Doroshenko, P. Koranda, H. Jelínková, J. Šulc, M. Němec, T.T. Basiev, V.K. Komar, A.S. Gerasimenko, and V.M. Puzikov, *Laser Phys. Lett.* **4**, 503–506 (2007).
- [16] H. Jelínková, P. Koranda, M.E. Doroshenko, T.T. Basiev, J. Šulc, M. Němec, P. Černý, V.K. Komar, and M.B. Kosmyna, *Laser Phys. Lett.* **4**, 23–29 (2007).
- [17] N.N. Il'ichev, P.V. Shapkin, E.S. Gulyamova, A.V. Kir'yanov, and A.S. Nasibov, *Laser Phys.* **20**, 1091–1094 (2010).
- [18] P.B. Meng, B.Q. Yao, G. Li, Y.L. Ju, and Y.Z. Wang, *Laser Phys.* **21**, 352–355 (2011).
- [19] C.H. Zhang, P.B. Meng, B.Q. Yao, G. Li, Y.L. Ju, and Y.Z. Wang, *Laser Phys.* **21**, 44–47 (2011).
- [20] I.S. Moskalev, V.V. Fedorov, and S.B. Mirov, *Opt. Express* **17**, 2048–2056 (2009).
- [21] M.E. Doroshenko, H. Jelínková, P. Koranda, J. Šulc, T.T. Basiev, V.V. Osiko, V.K. Komar, A.S. Gerasimenko, V.M. Puzikov, V.V. Badikov, and D.V. Badikov, *Laser Phys. Lett.* **7**, 38–45 (2010).
- [22] D.V. Shabanov, G.V. Geliknov, and V.M. Gelikonov, *Laser Phys. Lett.* **6**, 753–758 (2009).
- [23] A.K. Kodali, M. Schulmerich, J. Ip, G. Yen, B.T. Cunningham, and R. Bhargava, *Anal. Chem.* **82**, 5697–5706 (2010).
- [24] E.N. Benteil, W.-D. Li, J.X. Chen, A. Ritter, S. Chou, and C. Gmachl, in: *Proc. of the Conference on Lasers and Electro Optics*, San Jose, CA, USA, May 16–21, 2010 (CLEO 2010), paper CTuW4.
- [25] R.W. Wood, *Philos. Mag.* **4**, 396–402 (1902).
- [26] R. Petit (ed.), *Electromagnetic Theory of Gratings* (Springer-Verlag, Berlin, 1980), chap. 5.
- [27] G.A. Golubenko, A.S. Svakhin, V.A. Sychugov, and A.V. Tishchenko, *Sov. J. Quantum Electron.* **15**, 886–887 (1985).
- [28] I.F. Salakhutdinov, V.A. Sychugov, and O. Parriaux, *Quantum Electron.* **28**, 983–986 (1998).
- [29] J.A. Caird, M.D. Shinn, T.A. Kirchoff, L.K. Smith, and R.E. Wilder, *Appl. Opt.* **25**, 4294–4305 (1986).